JOURNAL OF CATALYSIS 138, 351–363 (1992)

Hydrodenitrogenation-Selective Catalysts

I. Fe Promoted Mo/W Sulfides

T. C. Ho, A. J. Jacobson,[1] R. R. Chianelli, and C. R. F. Lund[2]

Corporate Research Laboratories, Exxon Research and Engineering Company, Annandale, New Jersey 08801

Received April 3, 1992; revised June 3, 1992

This paper describes the development of a new catalyst system which gives an unusual combination of high hydrodenitrogenation and low hydrodesulfurization. This has been observed in tests with a highly aromatic distillate feed. The catalyst is an unsupported iron-promoted molybdenum or tungsten sulfide formed from thermal decomposition of bis(diethylenetriamine) iron thiomolybdate or thiotungstate. The results from a brief accelerated aging experiment have shown that this bulk sulfide system is thermally stable. Characterization of the Fe–Mo catalyst has indicated that it consists of a single sulfide phase which during activity testing partially transforms into an iron sulfide mixed with an MoS_2-like phase.

INTRODUCTION

In the face of mounting public concerns over environment and a dwindling supply of high-quality crudes, there is little doubt that hydroprocessing will become increasingly important in years to come. One can think of a scenario where future hydroprocessing processes will place great emphasis on catalyst selectivity. Among the reasons are [1] that hydrogen will become more costly, [2] that to remain competitive, refiners must become more and more efficient and flexible, and [3] that selective separation based on molecular type will play an increasingly important role in fuels/lubes processing. A major shortcoming of current commercial catalysts is that the hydrodenitrogenation (HDN) rate is relatively slow. Assertions have been made that to improve the HDN activity of conventional catalysts, one needs to first improve their hydrodesulfurization (HDS) activity.

In this paper we describe the development of a catalyst system which gives an unusual combination of high HDN and low HDS activity. This implies that enhancing HDS activity is not necessarily a prerequisite to enhancing HDN activity. In other words, nitrogen heteroatom is not necessarily more difficult to remove than sulfur heteroatom, although this is expected to be the case based on the carbon–heteroatom bond strength in aromatic systems. Fischer *et al.* (*1*) in their patient described how a high HDN-to-HDS ratio could be achieved with commerical catalysts by adding H_2S to the feed gas. Their results may be rationalized by the well-documented H_2S effect: H_2S can enhance HDN while inhibiting HDS (*2*, *3*, and references therein). Vít and Zdrăzil (*4*) have recently reported that certain noble metal sulfides are quite HDN selective. Their results were obtained by using model compounds (pyridine and thiophene) under relatively mild conditions.

The HDN-selective catalysts we report here are unsupported, low-surface-area iron-promoted molybdenum and tungsten sulfides generated by thermal decomposition of bis(diethylenetriamine) iron thiomolybdate and its tungsten analog (*5*, *6*). A heterometallic metal sulfur complex of this kind may be called *self-promoted,* since the

[1] Current address: Department of Chemistry, University of Houston, Houston, Texas 77204.

[2] Current address: Department of Chemical Engineering, State University of New York, Buffalo, New York 14260.

0021-9517/92 $5.00

primary and promoter metals are molecularly associated with each other in a single complex. Unlike commercial catalysts and the heterometallic metal oxygen complexes described in (*7, 8*), here the catalyst precursors are already in a sulfide form.

It should be pointed out that the use of iron as a hydroprocessing catalyst promoter is not new. British Petroleum's Ferrofining process, developed for upgrading lube oils (*9*), uses a supported Co–Mo catalyst promoted by a significant amount of iron (e.g, iron as oxide in the neighborhood of 10 wt%). Here the iron is used as a copromoter. In this regard, we mention that Ternan (*10*) has shown that using Fe alone as a promoter for molybdenum sulfide is not effective compared to Co or Ni.

The remainder of the paper is organized as follows. We first describe catalyst preparation. We then discuss the structure of the bulk catalysts based on information obtained from X-ray powder diffraction, transmission electron microscopy (TEM), and Mössbauer. Following this, the results from activity/selectivity tests are presented. Since the present bulk Fe–Mo and Fe–W sulfides represent a new catalyst system, we next address the question of its stability. Some remarks regarding the origin of the catalyst selectivity and possible practical applications are made in the final section.

CATALYST PREPARATION

Bulk Fe–Mo and Fe–W Catalysts

The catalyst precursors used in this study, called iron amine thiomolybdate and thiotungstate for short, have a well-defined coordinative structure. The synthesis of this class of compounds appears to date from the work of Spacu and Pop (*11*). The preparation of the Fe–Mo catalyst precursor is typically carried out as follows (*5, 6*):

Iron diethylenetriamine (dien) thiomolybdate $Fe(dien)_2MoS_4$ was prepared by dissolving 50 gm of $(NH_4)_2MoS_4$ into 82 ml of diethylenetriamine in a 1-liter flask. The resulting dark red solution was cooled to 0°C in an ice bath and kept in the bath for the duration of the experiment. In a separate flask, 42.84 gm of $FeCl_2 \cdot 4H_2O$ were dissolved into 250 ml of distilled H_2O, and at least 25 ml of diethylenetriamine was added slowly to this Fe^{2+} solution to form $Fe(dien)_2^{2+}$. The resulting brownish $Fe(dien)_2^{2+}$ solution was allowed to cool at room temperature. The $Fe(dien)_2^{2+}$ solution was then added slowly, as aliquots, to the $(NH_4)_2MoS_4$/dien solution with agitation for approximately 2 min after each addition. An orange-red precipitate formed immediately. Distilled H_2O was added to increase the volume of the reaction mixture. The mixture was kept in the ice bath for at least 15 min until the reaction was completed. The precipitate was separated out by vacuum filtration through a Buchner funnel. The product $Fe(dien)_2MoS_4$ was further washed with ethanol and dried under vacuum for 16–24 h; 93 gm of $Fe(dien)_2MoS_4$ were recovered.

Of course, the amine chelating ligand used in the above preparation does not have to be tridentate. Other chelating ligands can also be used (*5, 6*). The above procedure can be easily modified to prepare the bulk Fe–W sulfide.

Prior to use, the precursor compound is sulfactivated; that is, it is thermally decomposed to remove its organic constituents in the presence of a sulfur-bearing stream. We have found that this procedure is advantageous, even though the precursor compounds already have sufficient sulfur required for the formation of final working catalysts. The sulfur activation experiments were typically carried out as follows: The pelletized catalyst precursor was placed in a downflow fixed-bed reactor where it was purged for 1 h under nitrogen at 100°C and atmospheric pressure. Following this, a gas mixture containing 10% H_2S in H_2 was introduced into the reactor at a flow rate of 0.75 SCF/hr for each 10 cc of catalyst precursor in the reactor. The reactor temperature was then raised to 325°C and kept at this temperature for 3 h after which the reactor temperature was lowered to 100°C, the H_2S/H_2 gas flow was stopped, and the reactor was

purged with nitrogen until room temperature was reached. The catalysts were discharged from the reactor and then pressed into pellets and sized to 20–40 mesh granules. Note that the preparation does not involve calcination in air. In the conventional preparation, calcination often results in the formation of oxides and semisulfides even after severe sulfiding. Another point of note is that here the sulfur activation does not give rise to hot spotting. By contrast, gas sulfiding of conventional catalysts and self-promoted metallates is highly exothermic (*8, 12*).

Reference Catalysts

For comparison purposes two base-case catalysts were prepared. Both were prepared by skipping the amine complexing step. The first, denoted by $(Fe–Mo)_1$, was not supported on an oxide. Its preparation proceeded as follows: Forty grams of $FeCl_3$ was ground to a fine powder, and 26.1 g of $(NH_4)_6Mo_7O_{24}{\cdot}4H_2O$ were added under continued mixing until the mixture was homogeneous. Sufficient water was added until the mixture had a paste-like consistency. The product was dried overnight in a vacuum oven at 100°C, followed by calcining at 500°C for 4 h. The dark brown powder was pilled to 20–40 mesh particles with the aid of an aqueous 4% polyvinyl alcohol binding solution. Presulfiding of this catalyst was carried out with a 10/90 H_2S/H_2 mixture at 325°C for 3 h in the same manner as that described before.

The other base-case catalyst, denoted by $(Fe–Mo)_2$, was supported on γ-alumina. It was prepared as follows: 32.7g of $Fe(NO_3)_3 \cdot 9H_2O$ was dissolved in 75 ml of deionized water and the pH adjusted to 0 with about 2 ml HNO_3. This solution was used to impregnate 37.2g of γ-Al_2O_3. The resultant paste was dried overnight at 100°C and then calcined in air at 550°C for 4 h. The product was then treated with an aqueous solution of 8.76 g $(NH_3)_6Mo_7O_{24} \cdot 4H_2O$ which had been adjusted to pH = 14 with NH_4OH. The wet mass was again dried at 100°C overnight, followed by a 4-h calcination at 550°C. The golden brown product was crushed and screened to 20–40 mesh. Presulfiding was done at 325°C for 3 h with a 10/90 H_2S/H_2 stream in the usual manner.

TABLE 1

Properties of Commercial Catalysts

Catalyst	wt%			BET surface area (m^2/g)	Pore vol. (cc/g)
	MoO_3	CoO	NiO		
A	12.5	3.5	—	285	0.52
B	18.0	—	3.5	180	0.5
C	20.0	—	5.0	160	0.44

Three commercial catalysts, one Co–Mo and two Ni–Mo, were tested to provide another set of base cases. Their properties are listed in Table 1. These γ-Al_2O_3-supported catalysts were presulfided at 360°C and ambient pressure for 1 h with a 10% H_2S-in-H_2 gas mixture. Note that commercial Co–Mo catalysts are known to be less active and selective for HDN than their Ni–Mo counterparts. The inclusion of a Co–Mo catalyst here gives us some indication of the range of HDN selectivity with commercial catalysts.

CATALYST CHARACTERIZATION

The BET surface area of the bulk Fe-Mo catalyst after decomposition is quite low, about 2 m^2/g. The pore-size distribution is bimodal, with peaks at 30 and 6000 Å. The total pore volume is 0.41 cc/g, which is predominantly (>97%) contributed by the macropores (>100 Å).

X-ray Diffraction and TEM

X-ray diffraction (XRD) measurements were made using a Siemens D500 X-ray diffractometer. Figure 1a shows the powder diffraction pattern of *spent* bulk Fe–Mo catalyst after a 300-h on-oil activity test at 325°C. The catalyst was prepared from sulfiding $Fe(dien)_2MoS_4$ at 325°C. One sees a poorly crystalline MoS_2 (*13*) superimposed with four "sharp" lines of an iron sulfide phase identified as pyrrhotite (see Table 2).

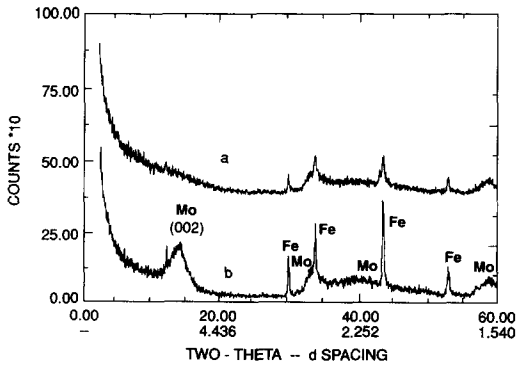

FIG. 1. (a) X-ray powder diffraction pattern of spent Fe–Mo catalyst after a 300-h activity test. (b) X-ray powder diffraction pattern of an unsupported Fe–Mo sulfide prepared from mixing $FeCl_2 \cdot 4H_2O$ and $(NH_4)_2MoS_4$ followed by sulfiding at 400°C.

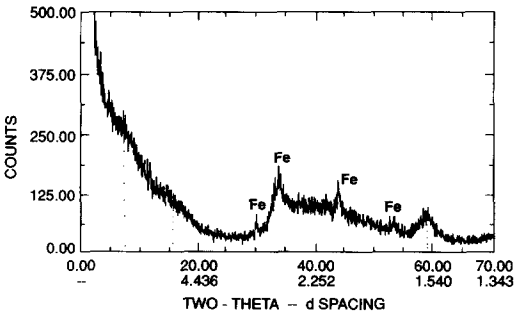

FIG. 2. X-ray powder diffraction pattern of $Fe(dien)_2MoS_4$ after sulfiding at 400°C.

No oxides were detected, despite the fact that the catalyst had been exposed to air for a brief period of time. For comparison, also shown in Fig. 1b is the diffraction pattern for an Fe–Mo bulk sulfide prepared from mixing 4.4 g $FeCl_2 \cdot 4H_2O$ and 5.76 g $(NH_4)_2MoS_4$ followed by sulfiding at 400°C for 2 h. One sees crystalline $Fe_{1-x}S$. The stacking of MoS_2, as indicated by the (002) peak at $2\theta = 14.4°$, is also quite noticeable. By contrast, Fig. 2 shows that the (002) peak is absent for the *fresh* bulk Fe–Mo sulfide prepared from sulfiding $Fe(dien)_2MoS_4$ at 400°C. Apparently, the use of the amine chelating ligand in the preparation suppresses the stacking of the MoS_2 phase even at 400°C. The presence of four "sharp" pyrrhotite peaks is due to the high sulfiding temperature used. When sulfided at 350°C or lower, the pyrrhotite peaks disappear, leaving only an amorphous phase.

TABLE 2

Lattice Parameters for Pyrrhotite $Fe_{1-x}S$ (ASTM 25-411)

(*hkl*)	*d*-Spacing (Å)
200	2.98
201	2.65
202	2.07
220	1.72

Figure 3 is a transmission electron micrograph of the *spent* Fe–Mo catalyst. This was obtained by using a high-resolution electron microscope (Philips EM-300) with a resolution of at least 2.5 Å. The straight lines on the right are the sharp lattice fringes of the pyrrhotite phase, while those on the left are "worm-like" lines which we believe are MoS_2 single and occasionally double layers or chains. That MoS_2 layer spacing is 6.15 Å allowed us to estimate the lattice spacing for the pyrrhotite phase, which is 5.8 ± 0.2 Å. This corresponds to such low-index planes as (100) and (010) of the pyrrhotite structure. This picture is consistent with the above XRD interpretation.

Mössbauer

In the Mössbauer experiments described here, only ^{57}Fe absorber studies have been made. The precursor compound used for Mössbauer characterization was treated at 350°C in a 15% H_2S in H_2 gas mixture. Figure 4 shows the Mössbauer spectrum of this catalyst which was handled in air during mounting on the spectrometer and during data collection. The figure includes spectra recorded at both room temperature (Fig. 4a) and at approximately 77°K (Fig. 4b). (The sample was mounted on a cold finger of a dewar filled with liquid N_2 and evacuated to ca. 10^{-3} mm Hg.) In both cases the data

FIG. 3. Transmission electron micrograph of spent Fe–Mo catalyst showing $Fe_{1-x}S$ and MoS_2-like phases.

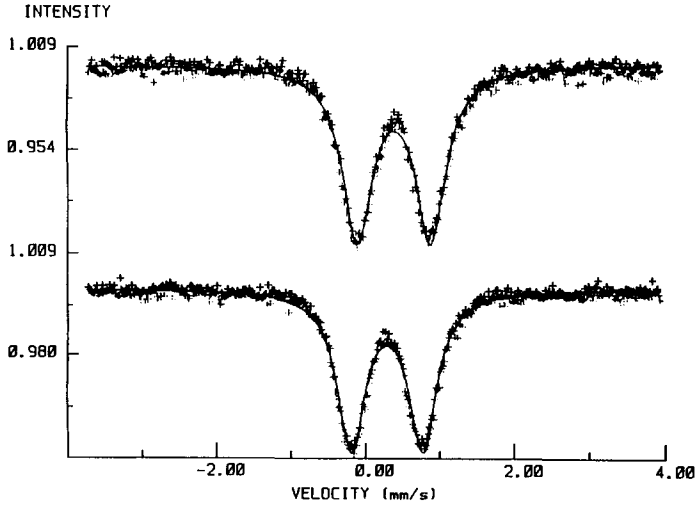

FIG. 4. Mössbauer spectra of unsupported iron–molybdenum sulfide prepared by decomposition of $Fe(dien)_2MoS_4$. Spectra recorded at room temperature (lower curve) and ca. 77 K (upper curve) are shown as + 's; the computer fit is shown as a solid line.

TABLE 3

Mössbauer Parameters for Fe–Mo and Co–Mo Catalysts

Material	Temperature (K)	δ (mm/s)	ΔE_Q (mm/s)	Γ (mm/s)
FeMoS	77	0.397	0.987	0.486
FeMoS	298	0.299	0.966	0.463
CoMoS(0.25)[a]	298	0.34	1.03	
CoMoS(ppm)[b]	298	0.32	1.21	

[a] Only the 80% of the Co present as CoMoS material is included in the table.

[b] CoMoS Mössbauer properties were taken from Ref. (*14*).

were fit using one spectral doublet with a Lorenzian lineshape. The two lines of the doublet were constrained to have equal intensity and width. The spectral parameters derived from the fit are summarized in Table 3. The first of these is the isomer shift (δ), which is a measure of the change in the electron density at the nucleus of the ^{57}Fe atoms in the sample relative to that in the ^{57}Fe atoms in the reference (metallic α-iron in the present study). Changes in the electron density at the nucleus are primarily associated with changes in the oxidation state of the iron. The second parameter is the quadrupole splitting, ΔE_Q. It is caused primarily by a nonspherical distribution of the electrons about the nucleus and to a lesser extent by the crystal field of the lattice. One final parameter is the linewidth, Γ, which is expected to be of the same magnitude as the natural linewidth of the state in question.

Topsøe *et al.* (*15*) showed Mössbauer absorption spectra of both bulk and supported sulfided Fe–Mo, but they did not present the Mössbauer parameters for the samples. The spectra are remarkably similar to those for sulfided Co–Mo materials. In what follows we compare our Mössbauer results with those of Topsøe *et al.* (*14*) for sulfided Co–Mo. Our conclusion is that the bulk catalyst prepared from $Fe(dien)_2MoS_4$, *prior to activity testing*, appears to be composed of an iron analog of the CoMoS material found by Topsøe *et al.* (*14*). This is elaborated as follows.

First, the iron in the Fe–Mo catalyst is not in any common iron sulfide phase, or any of the reported iron–molybdenum sulfides. Table 3 also includes Mössbauer parameters for the two CoMoS materials described in (*14*). The first CoMoS material was prepared by homogeneous precipitation and contains the metals in a Co/Mo ratio of approximately 0.25. For this material only the parameters reported for the CoMoS phase are included in Table 3, although the catalyst contained about 20% of its Co as Co_9S_8. The second CoMoS material was prepared by impregnation of MoS_2 with a cobalt salt solution. In this case the ratio Co/Mo is in the ppm regime. The parameters of the iron–molybdenum sulfide prepared by decomposition of $Fe(dien)_2MoS_4$ are quite similar to those of the CoMoS phase, more so than to those reported for iron or iron–molybdenum sulfides in the literature (*16–23*).

While comparison suggests that the freshly sulfided Fe–Mo catalyst is comprised of an FeMoS phase, there are nevertheless differences between this catalyst and the conventional CoMoS-containing catalysts. Indeed, in spite of the bulk Fe-to-Mo ratio of unity, the only iron-containing phase appears to be the FeMoS. With the CoMoS materials even at a low Co-to-Mo ratio of 0.25, a second Co_9S_8 phase was present. Figure 5 shows the spectrumn of an Fe–Mo catalyst prepared using a decomposition treatment at a higher temperature, that is, a pretreatment wherein some of the iron has separated from the FeMoS phase (*22*). In that case a pyrrhotite phase is clearly seen in the spectrum. How much of the single FeMos phase remains in the stable catalyst is unknown at this point.

The other differences between the unsupported Fe–Mo sulfide and the CoMoS materials are believed to be due to the higher promoter to molybdenum ratio of the former. For example, the quadrupole splitting of the iron catalyst is smaller than that of the CoMoS's. However, the trend indicated in Table 3 suggests that the higher the promoter metal concentration in the CoMoS phase, the lower the splitting, and therefore,

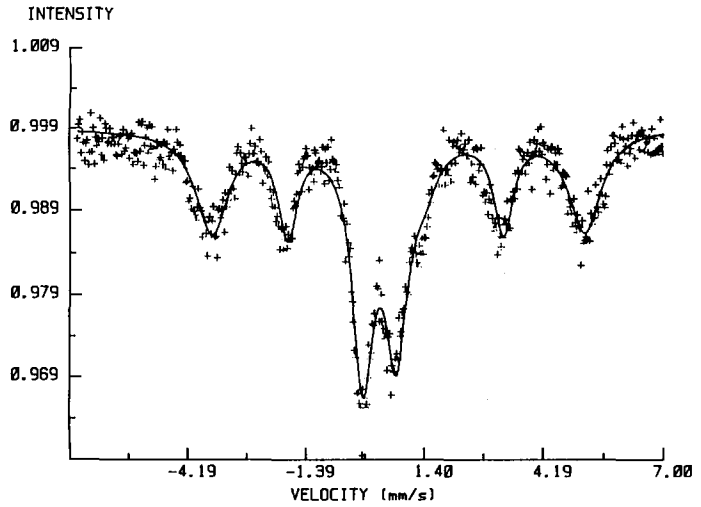

FIG. 5. Mössbauer spectrum of unsupported material where decomposition conditions were too severe. The spectrum was recorded at room temperature.

the still lower quadrupole splitting of the Fe–Mo catalyst may merely reflect the higher Fe-to-Mo ratio. The same reasoning may apply to the isomer shift, which could in addition be different simply because the phase is an FeMoS phase and not a CoMoS phase. Also, the changes observed in these two Mössbauer parameters when the temperature is varied are comparable in magnitude and sign to the changes reported for the CoMoS materials.

ACTIVITY AND SELECTIVITY TESTS

Feedstocks

Two light catalytic cycle oils, with an API gravity (at 60°F) of about 19, were used. Feedstock A contains 1.5 wt% total sulfur and 370 wppm total nitrogen. Feedstock B contains 1.25 wt% sulfur and 298 wppm nitrogen. The former was characterized in some detail. Its molecular types are as follows: Paraffins constitute about 20 wt%, with the remainder being homocyclic and heterocyclic aromatics. The distribution (wt%) within homocyclic aromatics is approximately 50% one-ring, 35% two-ring, and 15% three-ring. The sulfur compounds are almost exclusively of the benzo- and dibenzothiophene types, which split more or less evenly. About 70% of the nitrogen compounds are carbazoles and the other 30% are spread evenly between indoles and quinolines. Table 4 shows the GC distillation data.

Procedure

After presulfiding, the catalyst (typically 20 cc) was loaded into an automated trickle-bed unit consisting of several independent reactors disposed symmetrically in a common sand bath. Each reactor was equipped with a calibrated feed burette, pump, gas–liquid separator, and product liquid collector.

TABLE 4

GC Distillation of Feedstock A

wt%	Temp.(°C)
5	231
10	251
50	293
70	321
90	352
95	364

The reactor was packed with catalyst in the central zone and 1/16″ alundum in the fore and aft zones. All the hydroremoval rates were measured at a set of standard conditions: temperature, 325°C; pressure, 3.15 MPa; hydrogen treat gas, 3000 SCF/B; and LHSV (based on reactor volume), 1.5–6.0. The attainment of isothermal conditions was indicated by temperature measurement across the bed. After the break-in period (typically 30–50 h), the reaction was allowed to proceed for at least 20 h more before the first product sample was analyzed.

Analytical

After purging with nitrogen, the liquid products were analyzed for total sulfur by X-ray fluorescence using external standards and for total nitrogen by combustion and chemiluminescence using the Antek analyzer.

Data Analysis

Because of the excess of H_2, the H_2 concentration remains essentially constant throughout the catalyst bed. The H_2 concentration term can be incorporated into the rate constant of kinetic rate expression. Based on the Weisz–Prater criterion, we concluded that pore diffusion limitation is not likely under the test conditions employed. The mass balance equation for a pseudo-second-order reaction occurring in a plug-flow reactor is used to regress the HDS data; that is,

$$K_S = \text{LHSV}\left(\frac{1}{S_p} - \frac{1}{S_f}\right), \qquad (1)$$

where S is wt% of sulfur in the oil. The subscripts f and p refer to feed and product, respectively. For HDN, a first-order kinetics is used, viz.,

$$K_N = \text{LHSV} \ln\frac{N_f}{N_p}. \qquad (2)$$

The apparent rate constants can thus be determined by a least-squares fit to the data. For instance, K_S was calculated from the slope of a linear plot of $(S_f/S_p - 1)$ vs 1/LHSV. The fit was forced to pass through the origin. It must be emphasized that the rate constants so obtained represent the catalyst's volumetric activity. The bulk Fe–Mo catalyst has a packing density of about 1.1 g/cc, compared to 0.8 g/cc for the commercial catalysts.

TABLE 5

Summary of Catalyst Activity and Selectivity in Tests with Feedstock A

Catalyst	K_N	K_S	S_N
A	0.55	10.7	0.05
B	1.26	9.9	0.13
Fe–Mo	1.18	1.7	0.69
Fe–W	3.39	4.4	0.77
$(Fe–Mo)_1$	0.35	~ 0	~ 0
$(Fe–Mo)_2$	0.37	1.42	0.26

Note. K_N: cc oil/cc cat.·h; K_S: cc oil/cc cat.·h·wt%.

For a given feedstock, the selectivity of the catalyst for HDN relative to HDS, S_N, can be conveniently defined as the ratio of the rate constant of HDN to that of HDS,[3] that is,

$$S_N = \frac{K_N}{K_S}. \qquad (3)$$

Results

Table 5 summarizes the regression results obtained from tests with feedstock A. One can see that here the difference between the commercial Ni–Mo and Co–Mo catalysts mainly lies in their HDN activity. Within the range of conditions employed, the Ni–Mo catalyst is at least two times more selective than the Co–Mo catalyst for HDN.

The Fe–Mo catalyst prepared from Fe $(dien)_2MoS_4$, while having an HDN activity comparable to that of the commercial Ni–Mo catalyst (catalyst B), is about six times less active for HDS. The Fe–W

[3] Alternatively, one may use the dimensionless quantity, $S_N = K_N/(K_S S_f)$, as a measure of selectivity.

catalyst is more active and selective for HDN than the Fe–Mo catalyst. The two Fe–Mo base-case catalysts, $(Fe–Mo)_1$ and $(Fe–Mo)_2$, are both poor for HDN and HDS, indicating the importance of using an amine ligand in the preparation.

The results for the commercial catalysts explain why HDN has been perceived to be more difficult than HDS. For instance, with catalyst B (Ni–Mo on Al_2O_3), one can achieve only about 50% HDN but more than 90% HDS. However, the results for the bulk Fe–W catalyst apparently go against this "conventional wisdom" in that Fe–W shows a 2.7-fold (3.39 vs 1.26) HDN advantage over catalyst B. And this improvement is achieved at an HDS level less than half (4.4 vs 9.9) that attained by catalyst B. This suggests that nitrogen is no harder to remove than sulfur. In this regard, we remark that a kinetically important step in HDN and HDS of many multiring heterocycles is the hydrogenation of the heterocyclic ring. From the standpoint of resonance energy, there is no a priori reason why nitrogen heterocycles should be more difficult to hydrogenate than sulfur heterocycles (*3*). The challenge is how to develop a catalyst especially capable of attacking the organonitrogen compounds. The present catalyst system represents a step in this direction.

Another point to note is related to the H_2S effect. As mentioned, model-compound studies on commercial catalysts have found that H_2S formed from HDS can promote HDN. On the other hand, H_2S is known to inhibit HDS. Thus, in many cases a high HDN-to-HDS activity ratio can be obtained with a high H_2S-to-H_2 partial pressure ratio. From Table 5 one can see that the high HDN/HDS ratios of the bulk Fe–Mo and Fe–W catalysts were achieved without fortification of the gas with a high H_2S partial pressure. Thus, these bulk catalysts are inherently more selective toward HDN than commercial catalysts.

THERMAL STABILITY

As alluded to before, the present bulk sulfide system was prepared under thermally mild conditions (e.g, no calcination was used). A problem of central concern is its stability at severe reaction conditions. To address this question, we designed a set of accelerated aging experiments along the lines discussed in Ref. (*24*). Before proceeding further, we briefly discuss the rationale behind the experiments.

Accelerated Aging Experiments

Our primary concern here is the catalyst's intrinsic thermal stability. In order to generate an accelerated aging that is purely thermal in origin, the catalyst surface must see the same reactant concentration at the accelerated conditions as it sees at normal operating conditions. To meet this requirement, one can run the catalyst at a higher-than-normal temperature while maintaining constant conversion by operating at a higher space velocity. For a plug-flow reactor, this means that

$$\frac{K(T)}{\mathrm{LHSV}} = \text{constant}. \qquad (4)$$

Let $K(T) = A \exp(-E/RT)$, where A and E are the preexponential factor and activation energy, respectively. We then have

$$\ln(\mathrm{LHSV}) = -\frac{E}{RT} + \text{constant}. \qquad (5)$$

Since in general the activation energies for HDN and HDS are different, one cannot simultaneously maintain constant HDS and HDN at the high space velocity. So a compromise must be made. One way to do this is to choose a high temperature and a high space velocity so that the combined sulfur and nitrogen concentration at any point of the reactor under the accelerated conditions is *approximately* equal to that at normal conditions. This leads to the experimental design shown in Fig. 6, wherein ln(LHSV) is plotted against $1/T$ at 3.15 MPa and 3000 SCF H_2/B. The trajectories of constant HDS or HDN in this plot (isoconversionals) are straight lines with a slope equal to $-E/R$. For the Fe–Mo catalyst, the HDN and HDS isoconversionals are shown as

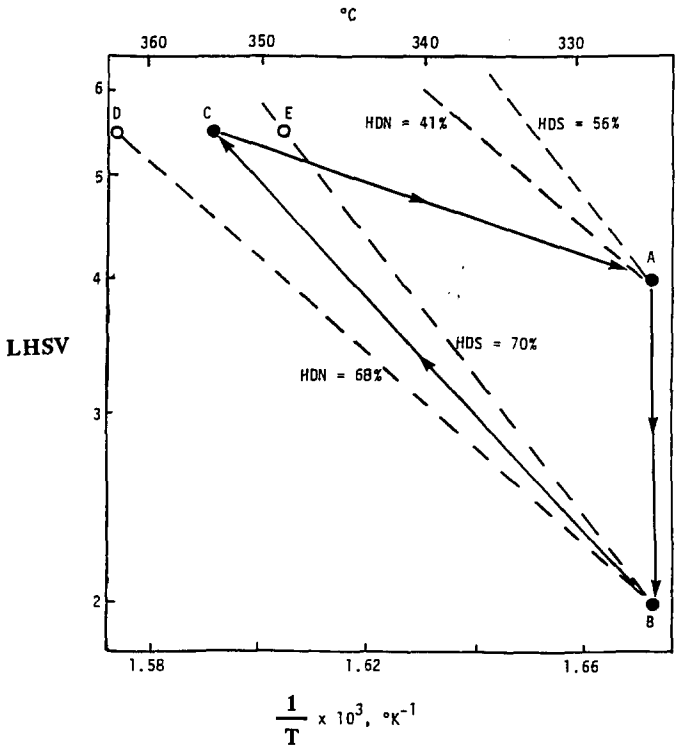

FIG. 6. Accelerated aging experiments via a pseudo-isoconversional policy for bulk Fe–Mo sulfide catalyst.

dotted lines in the figure (line BD for constant HDN and line BE for constant HDS). The experiments were conducted using feedstock B. The apparent activation energies for HDN and HDS are, respectively, 20 kcal/mol and 28.8 kcal/mol.

Specifically, the life test started off at the normal condition (325°C, 4.0 LHSV) to compare the selectivity and activity of the Fe-Mo catalyst to those of catalyst C, point A in Fig. 6. After 300 hours-on-stream, the LHSV was lowered to 2.0, while the temperature was held constant, point B. This condition was run for about 100 h. Subsequently, the temperature and LHSV were both increased to 355°C and 5.5, respectively, point C. This condition gives about twice the turnover rate as condition B while maintaining roughly the same total concentration of heteroatoms (*S* and *N*). The temperature here is much higher than that used in the catalyst preparation. Note that had condition D been used, the nitrogen concentration would have been identical to that given by condition B but the sulfur concentration would be much lower. A similar incompatible situation exists for condition E. Thus, condition C represents a reasonable compromise between conditions D and E. Line BC in Fig. 6 may thus be regarded as a *pseudo-isoconversional.* After being tested at condition C for about 100 h, the catalyst was again tested at condition A to check if there was any loss in selectivity or activity.

To summarize, the life test was bracketed by runs at condition A, and the sequence of the experiments is indicated by the arrows on the solid lines shown in Fig. 6.

Results of Accelerated Aging

Shown in Figs. 7 and 8 are, respectively, the HDN and HDS life data for the bulk

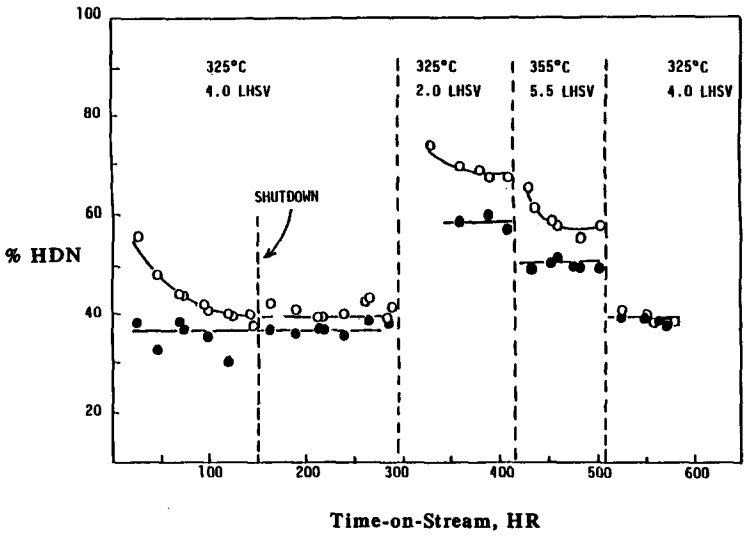

FIG. 7. HDN activity maintenance data for bulk Fe–Mo sulfide and catalyst C: open circles for Fe–Mo; solid circles for catalyst C.

Fe–Mo sulfide and catalyst C (which has a relatively high metal loading) using feedstock B. As can be seen, the Fe–Mo catalyst loses no activity or selectivity during the 600-h accelerated aging test. The initial HDN activity of the bulk catalyst is quite high. The catalyst needs about 100 h to line out its HDN activity but not its HDS activity. This could be due to strong adsorption of nitrogen compounds, rearrangement of catalyst surface, and/or crystallization. Table 6 summarizes the selectivity/activity comparison of the two catalysts evaluated. Thus, the Fe–Mo catalyst has an HDN ac-

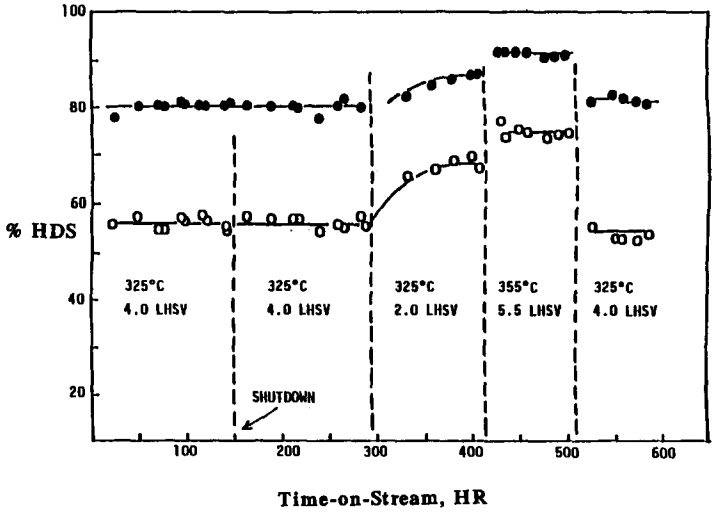

FIG. 8. HDS activity maintenance data for bulk Fe–Mo sulfide and catalyst C: open circles for Fe–Mo; solid circles for catalyst C.

TABLE 6

Selectivity/Activity Comparison, Feedstock B

	K_N		K_S		S_N	
	Fe–Mo	Cat C	Fe–Mo	Cat C	Fe–Mo	Cat C
325°C	2	1.9	5	17	0.41	0.11
355°C	4.5	3.9	16	51	0.29	0.08

tivity slightly higher than that of catalyst C. Due to its low HDS activity, the catalyst has approximately a 3.7-to-1 advantage in HDN selectivity over catalyst C. And this selectivity advantage shows little effect of temperature over 325–355°C. Note that for catalyst C, the HDN and HDS apparent activation energies are 17.8 and 27.2 kcal/mol, respectively. With either catalyst, S_N decreases with increasing temperature. This may be attributed to competitive adsorption and/or the higher activation energy for HDS than for HDN. Using the selectivity of the Fe–Mo catalyst at 325°C as a tie point, one can see that catalyst C is more HDN selective than catalyst B. This might be due to the high Ni-to-Mo ratio of the former.

CONCLUDING REMARKS

The bulk sulfide catalysts reported here, while showing respectable HDN activities, are quite selective for HDN compared with current commercial catalysts. They most likely provide more active sites for HDN, since the HDN activation energy with Fe–Mo is slightly higher than that with catalyst C. A prominent feature of the present catalyst system is the suppression of the stacking of MoS_2 layers. This may play a central role in determining the selectivity of the catalysts. Based on this, Daage and Chianelli (*25*) have proposed a geometrical model to rationalize the selectivity of MoS_2.

Being prepared from the decomposition of precursors containing an organic amine, these bulk catalysts invariably have some carbon- and nitrogen-containing species on their surfaces. These species may also be a contributing factor to the unusual selectivity observed. In this respect, we mention another highly active HDN catalyst system described in (*26*). The review by Prins *et al.* (*27*) contained a discussion of the desirability of having a carbonaceous species on catalyst surface. Model compound studies have indicated that molybdenum nitrides are active HDN catalysts (*28, 29*).

The results described in this paper indicate that there exists significant room for improving the HDN activity of commercial catalysts. The present catalyst system can be used for treating high nitrogen feedstocks. Also, its high HDN and low HDS activity suggests that it may be used in combination with an HDS-selective catalyst (e.g., Ref. (*30*)) in a two-stage process. The overall efficiency of such a process may well be very attractive because each reaction can be individually optimized. In any event, the development of a highly selective catalyst should give the refiners more freedom with respect to product properties and qualities. Although we have demonstrated in a short-term test (600 h) that the bulk Fe–Mo catalyst is thermally stable, long-term activity maintenance tests should be conducted.

REFERENCES

1. Fischer, R. H., Milstein, D., and Peters, A. W., U.S. Patent 3904513, assigned to Mobil Oil Corporation (1975).
2. Hanlon, R. T., *Energy Fuels* **1,** 424 (1987).
3. Ho, T. C., *Catal. Rev.-Sci. Eng.* **30,** 117 (1988).
4. Vít, Z., and Zdražil, M., *J. Catal.* **119,** 1 (1989).
5. Ho, T. C., Young, A. R., Jacobson, A. J., and R. R. Chianelli, U.S. Patent 4591429, assigned to Exxon Research and Engineering Co. (1986).
6. Jacobson, A. J., Ho, T. C., Chianelli, R. R., and

Pecoraro, T. A., U.S. Patent 4666878, assigned to Exxon Research and Engineering Co. (1987).
7. Ho, T. C., and McCandlish, L. E., U.S. Patent 4595672, assigned to Exxon Research and Engineering Co. (1986).
8. Ho, T. C., and Reyes, S. C., *Chem. Eng. Sci.* **45,** 2633 (1990).
9. Dare, H. F., and Demeester, J., Petroleum Refiner, Nov., p. 251 (1960). See also Demeester, J., U.S. Patent 3218251, assigned to British Petroleum Co. (1965).
10. Ternan, M., *J. Catal.* **104,** 256 (1987).
11. Spacu, G., and Pop, A., *Bull. Sect. Sci. Acad. Roum.* **21,** 188 (1938).
12. Reyes, S. C., and Ho, T. C., *AIChE J.* **34,** 314 (1988).
13. Chianelli, R. R., Prestridge, E. B., Pecoraro, T. A., and DeNeufville, J. P., *Science* **203,** 1105 (1979).
14. Topsøe, H., Clausen, B. S., Wivel, C., and Mørup, S., *J. Catal.* **68,** 433–52 (1981).
15. Topsøe, H., Clausen, B. S., Candia, R., Wivel, C. and Mørup, S., *Bull. Soc. Chim. Belg.* **90,** 1212 (1989).
16. Kjekahus, A., Nicholson, D. G., and Mukherjee, A. D., *Acta Chem. Scand.* **26**(3), 1105 (1972).
17. Morice, J. A., Rees, L. V. C., and Rickard, D. T., *J. Inorg. Nucl. Chem.* **31,** 3797 (1969).
18. Ono, K., Ito, A., and Hirahara, E., *J. Phys. Soc. Jpn.* **17,** 1615 (1962).
19. Coey, J. M. D., Spender, M. R., and Morrish, A. H., *Solid State Commun.* **8,** 1605 (1970).
20. Siller, A. H., McCormick, B. J., Russell, P., and Montano, P. A., *J. Am. Chem. Soc.* **100**(2), 2553 (1978).
21. Garg, V. K., Liu, Y. S., and Puri, S. P., *J. Appl. Phys.* **45**(1), 70 (1974).
22. Abe, M., Kaneta, K., and Uchino, M., *J. Phys. Soc. Jpn.* **44**(5), 1739 (1978).
23. Friedt, J. M., Dunlap, B. D., Shenoy, G. K., Aldred, A. T., Fradin, F. Y., and Kimball, C. W., *Physica* **107B,** 61 (1981).
24. Ho, T. C., *J. Catal.* **86,** 48 (1984).
25. Daage, M., and Chianelli, R. R., submitted for publication.
26. Seiver, R. L., and Chianelli, R. R., U.S. Patent 4540482, assigned to Exxon Research and Engineering Co. (1985).
27. Prins, R., DeBeer, V. H. J., and Somorjai, G. A., *Catal. Rev.-Sci. Eng.* **31,** 1 (1989).
28. Schllatter, J. C., Oyama, S. T., Metcalfe, J. E. III, and Lambert, J. M. Jr., *Ind. Eng. Chem. Res.* **27,** 1648 (1988).
29. Lee, K. S., Reimer, J. A., and Bell, A. T., *in* "ACS National Meeting, New York, August, 1991."
30. Halbert, T. R., Ho, T. C., Stiefel, E. I., Chianelli, R. R., and Daage, M., *J. Catal.* **130,** 116 (1991).